J Solid State Electrochem (2012) 16:2211–2216
DOI 10.1007/s10008-012-1649-z

ORIGINAL PAPER

A hydrogen peroxide biosensor based on the direct electron transfer of hemoglobin in the nanosheets of exfoliated HNb_3O_8

Yu-Ge Liu · Chang-bin Wei · Ling-Ling Lv · Sheng-Hui Liu

Received: 13 September 2011 / Revised: 2 January 2012 / Accepted: 5 January 2012 / Published online: 21 January 2012

Abstract In the present work, hemoglobin (Hb) was entrapped into the nanosheets of a pre-exfoliated layered material HNb_3O_8. UV–vis spectra analysis displayed that no significant denaturation occurred to the entrapped protein. Electrochemical results showed that the entrapment of Hb into layered HNb_3O_8 enhanced the direct electron transfer ability between protein molecules and electrode. A pair of well-defined redox peaks was observed at −0.39 and −0.34 V on the glassy carbon electrode modified with the Hb/HNb_3O_8 composite. The electrode reactions showed a surface-controlled process with a single electron transfer at the scan rate of 50–400 mV/s, and the electron transfer rate was very fast. The entrapped Hb retained its biological activity well and the sensor constructed by the Hb/HNb_3O_8-composite-modified electrode displayed excellent response to the reduction of hydrogen peroxide (H_2O_2) with wide linear range, low detection limit, and good stability.

Keywords Hemoglogin · Direct electron transfer · Layered HNb_3O_8 · Hydrogen peroxide · Biosensor

Introduction

The determination of hydrogen peroxide (H_2O_2) is of great importance in many fields, such as food, pharmaceutics, industry, clinical laboratory, and so on [1, 2]. Numerous quantitative methods have been developed for the detection of H_2O_2. The most commonly used approaches include spectrometry [3, 4], chemoluminescence [5–7], and amperometry [8–10]. However, these methods are either time-consuming or require expensive reagents and equipments. In recent years, much attention has been paid to the amperometric detection of H_2O_2 due to its simplicity, high selectivity, and high sensitivity [11–13]. This was generally based on the sensors constructed from the direct electrochemistry of proteins and enzymes.

Proteins are promising candidates for catalysts and sensors due to their excellent properties with super chemo-, regio-, and stereo-selectivity [14]. The electrochemical biosensors for the detection of H_2O_2 constructed on the basis of the direct electron transfer between redox proteins and the electrode surface have been increasingly developed in the fields of medicine, biotechnology, environmental monitoring, and so on [15–17].

Hemoglobin (Hb), the main component of red blood cells, is a soft globular heme protein. It has four electroactive iron hemes, a molar mass of approximately 64,500 g mol^{-1}, and a protein dimension of 5.3×5.4×6.5 nm [18]. This protein is often used as a model molecule for the study of the direct electron transfer between heme proteins and electrode surface because of its commercial availability and relatively well-known structure. It is also a most commonly used protein in the development of enzyme-based H_2O_2 biosensors [19–22].

Since the adsorption of protein molecules onto bare electrode surface may lead to their denaturation, which also decreases direct electron transfer rate and the efficiency for detecting H_2O_2, immobilization of proteins on supports is needed to display their special properties.

Immobilization on supports permits highly selective properties to be performed for proteins. Recently, layered materials have attracted great attention for their application in the immobilization of proteins and detection of H_2O_2. The "flexible pores" and the interlayer galleries in layered materials can be used to hold the dimension of guests, which makes them quite suitable to immobilize proteins with different dimensions

Y.-G. Liu (✉) · C.-b. Wei · L.-L. Lv · S.-H. Liu
South Subtropical Crops Research Institute,
Chinese Academy of Tropical Agricultural Science,
Zhanjiang 524091, China
e-mail: liuyugehb@sina.com

[21]. Different kinds of layered materials have been reported as supporting matrices for proteins, such as layered manganese oxide [23], layered niobate $HCa_2Nb_3O_{10}$ [24, 25], layered polysilicate magadiite [26], layered titanate [27], and layered phosphates [28–30].

HNb_3O_8 is a layered material synthesized by replacing the alkaline metal cations of KNb_3O_8 with H^+ through ion-exchange reactions. This material was mostly investigated in the field of semiconductor and photochemical catalysis [31, 32], or for the synthesis of polymer nanocomposite [33, 34]. Unlike other layered materials, such as layered niobate $HCa_2Nb_3O_{10}$ and layered phosphates, which have been extensively investigated for its application in biosensors and the realization of direct electron transfer, there have been no papers about the application of HNb_3O_8 in electrochemistry as far as we know. Based on the similarity of it structure to $HCa_2Nb_3O_{10}$ or other niobates, HNb_3O_8 should also posses such potential use. Therefore, the investigation in biosensors of HNb_3O_8 is of great importance for expanding its and other layer materials' new application.

In the present work, HNb_3O_8 was pre-exfoliated into platelets and used to immobilize hemoglobin for the construction of a sensor detecting H_2O_2. The direct electron transfer between the electrode and the protein was realized. The immobilized Hb exhibited a pair of well-defined peaks at wide scan rates, and the sensor fabricated displayed fast amperometric response, low detection limit, and good stability for the detection of H_2O_2.

Experimental

Reagents

Bovine heart Hb was purchased from Sigma and used without further purification. Tetrabutylammonium hydroxide (TBAOH) aqueous solution (10 wt.%) was purchased from Shanghai Chemical Reagent Co., Ltd. Hydrogen peroxide (H_2O_2, 30 wt.% solution) was obtained from Shanghai Biochemical Reagent Co., Ltd. All the other reagents are of analytical grade and used as received. Ultra-pure water was used for the preparation of solutions.

Synthesis and exfoliation of HNb_3O_8

KNb_3O_8 was prepared according to the procedure described before [35]. The proton-exchange reaction of KNb_3O_8 in 6 M nitric acid at room temperature resulted in the corresponding layered acidic material HNb_3O_8. The exfoliation of HNb_3O_8 was conducted by adding 10 wt.% TBAOH solution to 50 mL of distilled water containing HNb_3O_8. The solution was stirred at room temperature for 24 h and used without further treatment.

Entrapment of Hb and fabrication of biosensor

For the entrapment of Hb, stock solution of the protein (2 mg/mL, 0.1 M phosphate buffer solution (PBS), pH 7.0) and the exfoliated HNb_3O_8 (HNb_3O_8-e)were mixed together in a 1:1 volume ratio. The mixture was equilibrated for 24 h at room temperature and the resulted suspension was directly used for further test.

Glass carbon electrode (GCE) was polished with 1.0, 0.3 and 0.05 μm alumina powder successively, followed by rinsing thoroughly with ultra-pure water. The polished electrode was then sonicated in acetone and ultra-pure water and finally allowed to dry at room temperature. Ten microliters of the suspension of Hb/HNb_3O_8 achieved above was deposited onto the electrode surface. The electrode was then left to dry at 4 °C for at least 24 h. The sensor was stored under the same condition when not used.

Apparatus and measurements

Powder X-ray diffraction (XRD) patterns were obtained on an ARL X'TRA X-ray diffractometer using CuKα radiation. Scanning electron microscope (SEM) images were taken on Nova NanoSEM 230 field emission microscope. UV–vis absorption spectra were recorded on a Shimadzu UV-2401PC spectrophotometer. Cyclic voltammetric and amperometric experiments were conducted with a CHI660B workstation (Shanghai Chenhua, Shanghai). All experiments were carried out using a conventional three-electrode system, where GCE modified with Hb/HNb_3O_8 as working electrode, a platinum wire as auxiliary electrode and a saturated calomel electrode as reference electrode. All solutions were deoxygenated by highly pure nitrogen before and during the measurements.

Results and discussion

XRD and SEM analysis

The XRD pattern of HNb_3O_8 was given in Fig. 1a. The interlayer space of the material was calculated to be 1.09 nm according to the pattern. From the SEM image (Fig. 1b and inset), it can be clearly seen that the synthesized material possessed a typical layered structure.

UV–vis absorption spectroscopic analysis

UV–vis spectroscopy is a useful tool for monitoring the possible change of Soret absorption band in the heme group region [36]. The band shift may provide some information for the possible denaturation of heme protein, particularly that

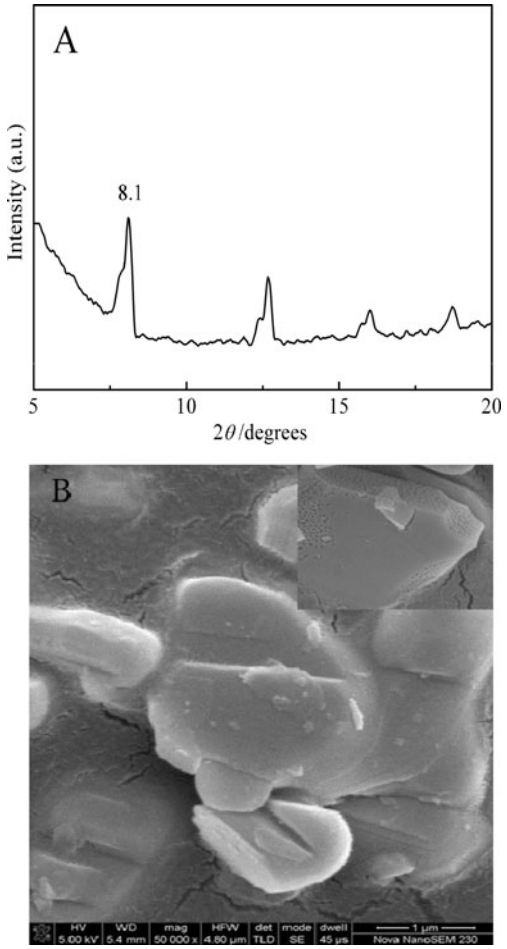

Fig. 1 XRD pattern (**A**) and SEM (**B**) of HNb_3O_8, *Inset* of **B**: A side view image of the layered material

of conformational change. Shown in Fig. 2 were the UV–vis spectra of pre-exfoliated HNb_3O_8, Hb/HNb_3O_8, and Hb solutions in 0.1 M PBS 7.0, respectively. It can be clearly seen that free Hb (curve a) and Hb/HNb_3O_8 (curve b) have Soret absorptions at 405 and 408 nm, while there was no adsorption appeared in the pre-exfoliated HNb_3O_8 UV–vis spectrum. The shift of the adsorption may be due to the tiny denaturation when the protein solution mixed with the strong alkaline solution of exfoliated HNb_3O_8, and the decrease in adsorption could be ascribed to different concentration of Hb in the Hb solution and the Hb/HNb_3O_8 composite.

Direct electrochemistry of Hb/HNb_3O_8-modified electrode

The cyclic voltammograms (CVs) of different electrodes at 100 mV/s are given in Fig. 3. There were no peaks at the electrode modified by pre-exfoliated HNb_3O_8 (curve b), indicating that HNb_3O_8 was inelectroactive in the area discussed. When the electrode was modified with only Hb (curve a), a couple of small peaks were observed, and the reduction current decreased with cycle numbers, suggesting that direct electron transfer was quite difficult between Hb and electrode without supports. However, a pair of well-defined redox peaks was observed at the Hb/HNb_3O_8-modified electrode at −0.39 and −0.34 V. These peaks were located much close to the characteristic potential of the heme Fe_{III}/Fe_{II} couples of the proteins in the literature [37]. The results above presented strong evidence that the direct electron transfer between Hb and GCE was achieved after combination with HNb_3O_8, and the immobilization may have more favorable orientation and facilitate the direct electron transfer between Hb and electrode.

The CVs of the Hb/HNb_3O_8-modified electrode displays a well-defined peak shape at different scan rates from 50 to 400 mV/s (Fig. 4). With the increase of scan rate, the redox peak currents of the Hb increased linearly, and also was the peak-to-peak separation (inset of Fig. 4), indicating a surface-controlled process.

For thin-layer electrochemistry, integration of CV peak can give the total amount of charge (Q) passed through the electrode for reduction or oxidation of electroactive species in the

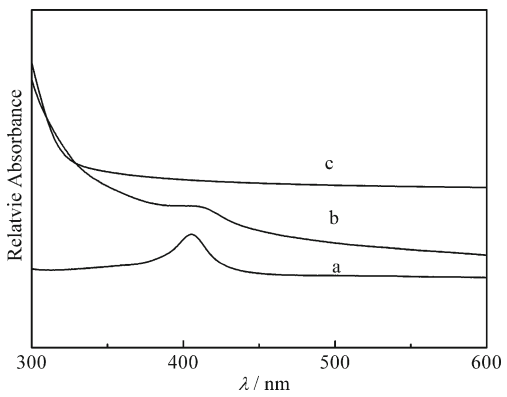

Fig. 2 UV–vis spectra of *a* Hb, *b* Hb/HNb_3O_8, and *c* pre-exfoliated HNb_3O_8 in 0.1 M PBS 7.0

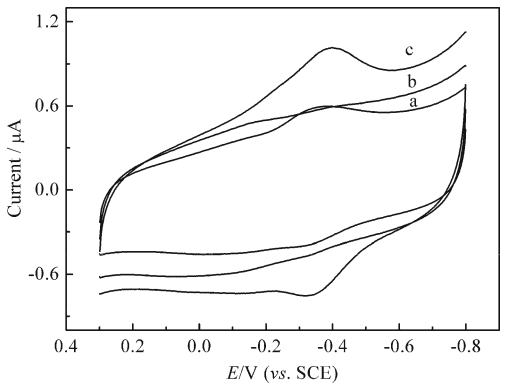

Fig. 3 Cyclic voltammograms of *a* Hb, *b* pre-exfoliated HNb_3O_8, and *c* Hb/HNb_3O_8-composite-modified electrode at 100 mV/s in 0.1 M PBS 7.0

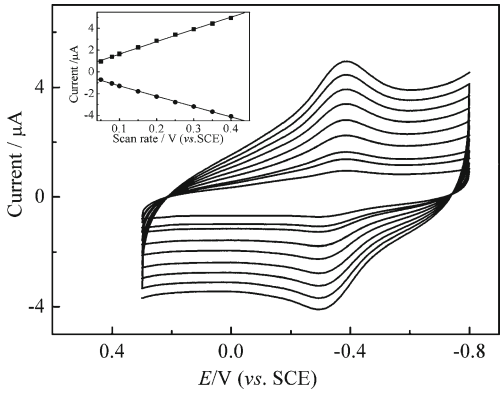

Fig. 4 Cyclic voltammograms of Hb/HNb_3O_8-composite-modified electrode in 0.1 M PBS 7.0 at 50, 80, 100, 150, 200, 250, 300, 350, and 400 mV/s (from inner to outside). *Inset* plot of peak current vs. scan rate

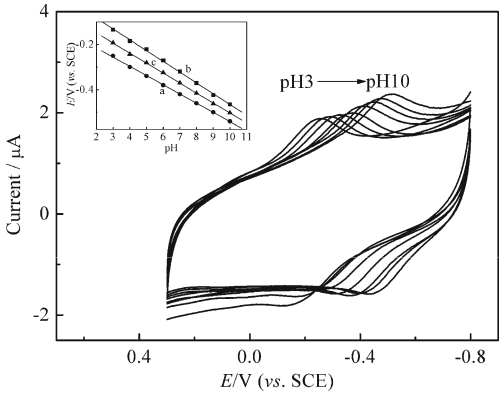

Fig. 5 Cyclic voltammograms of Hb/HNb_3O_8-composite-modified electrode in 0.1 M PBS with different pH values at 200 mV/s. *Inset* plots of pH vs. *a* cathodic, *b*, anodic and *c* formal potential ($E^{0\prime}$)

thin film. Its surface concentration (Γ^*) can be calculated from the Faraday's law:

$$\Gamma* = Q/nFA$$

Where n is the number of electrons transferred, F is Faraday's constant, and A is the electrode area. The average surface coverage of Hb calculated from Faraday's law is 1.25×10^{-10} mol/cm^2 for the Hb/HNb_3O_8-modified GCE. The value is larger than the theoretical monolayer coverage of Hb (ca. 1.89×10^{-11} mol/cm^2) on the basis of its crystallographic dimensional structure, assuming the biomolecule adopts an orientation with the long axis parallel to the electrode surface [38].

Small peak-to-peak separation always indicates a fast electron transfer rate. The electron transfer rate constant k_s can be estimated by the Laviron equation [39]:

$$\log K_s = \alpha\log(1-\alpha) + \alpha(1-\alpha)\log\alpha - \log\frac{RT}{nF\nu} - \frac{\alpha(1-\alpha)nF\Delta E_p}{2.3RT}$$

Where α is the charge-transfer coefficient, R the gas constant, T the absolute temperature, ΔE_p the peak potential separation, and v the scan rate. A graph of the peak potential versus the logarithm of the scan rate yields a straight line, from the slope a charge-transfer coefficient of 0.83 was estimated for Hb. The peak-to-peak separations were 64, 68, 76, 85, and 97 mV at the scan rate of 100, 150, 200, 250, and 300 mV/s, giving an average K_s value of 2.13±0.3 s^{-1}. The value was much larger than those reported [30, 39].

Influence of solution pH

In most cases, the pH values of solutions are very essential to the electrochemical behaviors of proteins. In this research, the Hb/HNb_3O_8-modified electrode showed strong dependence on solution pH. All the changes in the peak potential and current caused by pH (from 3.0 to 10.0) were reversible (Fig. 5). For example, the cyclic voltammogram for the Hb/HNb_3O_8 at pH 9.0 was reproduced after immersion in pH 4 buffer and then returned to the pH 9.0 buffer. The anodic, cathodic, and formal potential ($E^{0\prime}$) for the Hb/HNb_3O_8 electrodes showed a linear relationship with pH in a wide range of 3.0 to 10.0 with slopes of −47.71, −40.83, and −44.27 mV

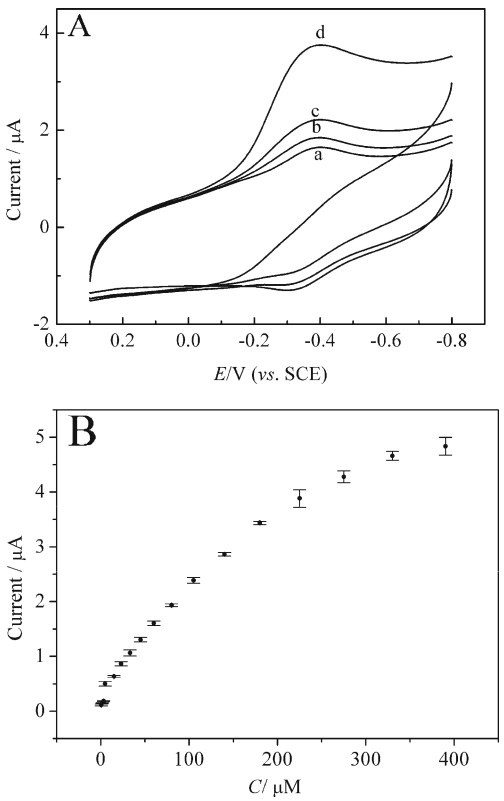

Fig. 6 **a** Cyclic voltammograms of Hb/HNb_3O_8-composite-modified electrode without (*a*) and with *b* 1×10^{-5} M, *c* 2×10^{-5} M, and *d* 1×10^{-4} M of H_2O_2 at 100 mV/s in 0.1 M PBS 7.0. **b** Calibration curve of current vs. H_2O_2 concentration

pH^{-1} (inset of Fig. 5), suggesting that there was nearly one electron participated in the electron transfer process. Thus, the reaction equation for the electrochemical reduction of Hb may be described as follows [40]:

$$\text{Hb heme Fe(III)} + H^+ + e^- \rightarrow \text{Hb heme Fe(II)}$$

Electrocatalytic reduction to H_2O_2 by the Hb/HNb_3O_8-modified electrode

Heme proteins have peroxidase activity and can be used to reduce hydrogen peroxide through electrochemical catalysis on the electrode, which means a biosensor for detecting H_2O_2 can be fabricated because of the property of Hb. Based on the excellent electrochemical behaviors of Hb/HNb_3O_8 discussed above, it was immobilized on the surface of GCE and applied to construct a sensor to detect H_2O_2.

The CVs of Hb/HNb_3O_8-modified electrode in 0.1 M pH 7.0 PBS before and after the addition of H_2O_2 are given in Fig. 6a. It can be seen that the reduction peak current increased and the anodic peak current decreased dramatically with the addition of H_2O_2 on the Hb/HNb_3O_8-modified electrode. Besides, the currents of the reduction peaks increased with the increase of H_2O_2 concentration, indicating a typical electrocatalytic reduction process. The reduction peak currents were in line with the concentration of H_2O_2 within the range of 5–180.1 μM with a detection limit of 1.5 μM (N=10; R=0.996; Fig. 6b). The relative standard deviation of the peak current in six successive determinations at a H_2O_2 concentration of 50 μM was 3.52% for Hb/HNb_3O_8-modified GCE.

The apparent Michaelis–Menten constant K_m^{app}, which gives an indication of the enzyme-substrate kinetics, is generally used to estimate the biological activity of immobilized enzyme. This constant was calculated by Lineweaver–Burk equation [41]:

$$1/I_{ss} = 1/I_{max} + K_m^{app}/I_{max}C$$

Where I_{ss} is the steady current after the addition of substrate (which can be obtained from amperometric experiments), C is the bulk concentration of the substrate, and I_{max} is the maximum current measured under the saturated substrate condition. The apparent Michaelis–Menten constant was calculated to be 91 μM for the Hb/HNb_3O_8-composite-modified electrode from the cyclic voltammograms when different concentration of H_2O_2 was added. This value was much smaller than 1,076 μM of the Hb–PHB-film-modified electrode [18], 710 μM of the Hb–$HCa_2Nb_3O_{10}$-modified electrode [25], and 340 μM of the Nafion–RTIL–Hb–MWNTs-modified electrode [42], suggesting a higher affinity and enzymatic activity to the reduction of H_2O_2.

Additional experiments were carried out to test the reproducibility and stability. No obvious change was found after the Hb/HNb_3O_8-modified electrode was immersed in PBS and stored in the refrigerator at 4 °C for 20 h. The biosensor could keep 90% of its initial response to H_2O_2 in a dry state at 4 °C within 2 weeks.

Conclusions

A sensor for detecting H_2O_2 was fabricated by entrapping Hb into the nanosheets of exfoliated HNb_3O_8. The direct electron transfer between Hb and the electrode was realized by dropping the resulted suspension onto the surface of electrode. The layered material provided an excellent support for Hb on the electrode and the entrapped protein remained its bioactivity well at a wide pH range. The sensor constructed showed fast detection to the reduction of with a wide linear range and low detection limit. This provides a facile way for the detection of H_2O_2 and realization of direct electron transfer direct electron between proteins and electrode.

Acknowledgments The work is supported by the Fund on Basic Scientific Research Project of Nonprofit Central Research Institutions (no. SSCRI200901), and the Natural science Foundation of Hainan province (no. 310099).

References

1. Kafi AKM, Ahmadalinezhad A, Wang J, Thomas DF, Chen A (2010) Biosens Bioelectron 25:2458–2463
2. Modrzejewska B, Guwy AJ, Dinsdale R, Hawkes DL (2007) Water Res 41:260–268
3. Chang Q, Zhu LH, Jiang GD, Tang HQ (2009) Anal Bioanal Chem 395:2377–2385
4. Srikun D, Albers AE, Nam CI, Iavaron AT, Chang CJ (2010) J Am Chem Soc 132:4455–4465
5. Chen WW, Li BX, Xu CL, Wang L (2009) Biosens Bioelectron 24:2534–2540
6. Zhang ZY, Zhang SC, Zhang XR (2005) Anal Chim Acta 541:37–47
7. Qin W, Zhang ZJ, Li BX, Liu SN (1998) Anal Chim Acta 372:357–363
8. Hanaoka S, Lin J, Yamada M (2001) Anal Chim Acta 426:57–64
9. Nakabayashi Y, Yoshikawa H (2000) Anal Sci 16:609–613
10. Kausaite-Minkstimiene A, Mazeiko V, Ramanaviciene A, Ramanavicius A (2010) Biosens Bioelectron 26:790–797
11. Wang J, Musameh M, Lin Y (2003) J Am Chem Soc 125:2408–2409
12. Matos RC, Pedrotti JJ, Angnes L (2001) Anal Chim Acta 441:73–79
13. Yao SJ, Xu JH, Wang Y, Chen XX, Xu YX, Hu SS (2006) Anal Chim Acta 557:78–84
14. Bornscheuer UT (2003) Angew Chem Int Ed 42:3336–3337
15. Armstrong F, Heering HA, Hirst J (1997) Chem Soc Rev 26:169–179
16. Willner I, Katz E (2000) Angew Chem Int Ed 39:1181–1218

17. Gooding JJ, Wibowo R, Liu JQ, Yang WR, Losic D, Orbons S, Mearns FJ, Shapter JG, Hibbert DB (2003) J Am Chem Soc 125:9006–9007
18. Peng S, Gao Q, Wang Q, Shi J (2004) Chem Mater 16:2675–2684
19. Wei N, Xin X, Du J, Li J (2011) Biosens Bioelectron 26:3602–3607
20. Zhang C, Liu M-C, Li P, Xian Y-Z, Cheng Y-X, Zhang F-F, Wang X-L, Jin L-T (2005) Chin J Chem 23:144–148
21. Sun W, Li X, Wang Y, Zhao R, Jiao K (2009) Electrochim Acta 54:4141–4148
22. Yu J-J, Zhao F-Q, Zeng B-Z (2008) J Solid State Electrochem 12:1167–1172
23. SchÖllhorn B (1996) Chem Mater 8:1747–1757
24. Gao Q, Suib S.L, Rusling JF (2002) Chem Commun 19:2254–2255
25. Gao L, Gao Q (2007) Biosens Bioelectron 22:1454–1460
26. Gao L, Gao Q, Wang Q, Peng S, Shi J (2005) Biomaterials 26: 5267–5275
27. Zhang L, Zhang Q, Lu X, Li J (2007) Biosens Bioelectron 23:102–106
28. Geng LN, Li N, Dai N, Wen XF, Zhao FL, Li KA (2003) Colloid Surf B 29:81–88
29. Kumar CV, Chaudhari A (2003) Microporous Mesoporous Mater 57:181–190
30. Liu Y, Lu C, Hou W, Zhu J-J (2008) Anal Biochem 375:27–34
31. Takagaki A, Sugisawa M, Lu D, Kondo JN, Hara M, Domen K, Hayashi S (2003) J Am Chem Soc 125:5479–5485
32. Liu JF, Li XL, Li YD (2003) J Cryst Growth 247:419–424
33. Yang G, Hou W, Feng X, Xu L, Liu Y, Wang G, Ding W (2007) Adv Funct Mater 17:401–412
34. Yang G, Liu Y, Hou W, Ji H, Li Y (2009) J Appl Poly Sci 113:78–86
35. Dion M, Ganne M, Tournoux M (1981) Mater Res Bull 16:1429–1435
36. Theorell H, Ehrenberg A (1951) Acta Chem Scand 5:823–848
37. Wang SF, Chen T, Zhang Z, Shen XC, Lu ZX, Pang DW, Wong KY (2005) Langmuir 21:9260–9266
38. Laviron E (1979) J Electroanal Chem 101:19–28
39. Xian Y, Zhou L, Wu F, Ling Y, Jin L (2007) Electrochem Commun 9:142–148
40. Trushina E, Oda R, Landers J, Mcmurray C (1997) Electrophoresis 18:1890–1898
41. Kamin RA, Wilson G (1980) Anal Chem 52:1198–1205
42. Zhang Y, Zheng J (2011) Chin J Chem 29:685–690